RSC Advances

This is an *Accepted Manuscript*, which has been through the Royal Society of Chemistry peer review process and has been accepted for publication.

Accepted Manuscripts are published online shortly after acceptance, before technical editing, formatting and proof reading. Using this free service, authors can make their results available to the community, in citable form, before we publish the edited article. This *Accepted Manuscript* will be replaced by the edited, formatted and paginated article as soon as this is available.

You can find more information about *Accepted Manuscripts* in the Information for Authors.

Please note that technical editing may introduce minor changes to the text and/or graphics, which may alter content. The journal's standard Terms & Conditions and the Ethical guidelines still apply. In no event shall the Royal Society of Chemistry be held responsible for any errors or omissions in this *Accepted Manuscript* or any consequences arising from the use of any information it contains.

ROYAL SOCIETY OF CHEMISTRY

www.rsc.org/advances

(Manuscript for *RSC advances*)

A versatile gold cross-linked nanoparticle based on triblock copolymer as the carrier of doxorubicin

Sangmin Jeon,‡[a] Hyewon Ko,‡[b] Vijayakameswara Rao N,[a] Hong Yeol Yoon,[a]

Dong Gil You,[a] Hwa Seung Han,[a] Wooram Um,[b] Gurusamy Saravanakumar,[a]

and Jae Hyung Park*[ab]

[a]School of Chemical Engineering, College of Engineering, Sungkyunkwan University, Suwon 440-746, Republic of Korea

[b]Department of Health Sciences and Technology, SAIHST,Sungkyunkwan University, Suwon 440-746, Republic of Korea

[c]

‡These authors contributed equally to this work

*Corresponding author:

Jae Hyung Park, Ph.D.

School of Chemical Engineering

College of Engineering

Sungkyunkwan University, Suwon 440-746, Republic of Korea

Tel: +82-31-290-7288; fax: +82-31-299-6857; e-mail: jhpark1@skku.edu

RSC Advances Accepted Manuscript

Abstract

In an attempt to develop biostable nanoparticles (NPs) as potential carriers of anticancer drugs, we prepared a triblock copolymer that can self-assemble into NPs and be gold cross-linked in aqueous conditions. The triblock copolymer, composed of poly(ε-caprolactone)-*block*-poly(2-(dimethylamino) ethyl methacrylate)-*block*-poly(ethylene glycol) (PCL-*b*-PDMAEMA-*b*-PEG), was synthesized by a combination of ring-opening polymerization, atom transfer radical polymerization and click chemistry. The chemical structures and compositions of the triblock copolymer and its intermediates were characterized by FT-IR and ^{1}H NMR. The triblock copolymer formed spherical NPs (195 nm in diameter) in PBS (pH 7.4). The anticancer drug, doxorubicin (DOX), was loaded into the NPs using a dialysis method. Tertiary amine groups, present in the PDMAEMA block of the triblock polymer, were used for *in situ* gold cross-linking, which was confirmed using transmission electron microscopy and UV/VIS spectroscopy. Bare NPs released 80% of DOX over 6 days, whereas only 40% of the DOX was released from gold cross-linked NPs (GNPs), implying that the gold cross-links act as a diffusion barrier of DOX. Owing to the slow release of DOX, the cytotoxicity of DOX-GNPs was much lower than that of DOX-loaded bare NPs. The blood concentrations of DOX were also monitored after intravenous injection of free DOX and DOX-loaded NPs into the tail veins of rats. The results indicated that the blood circulation time of DOX was longest for DOX-GNP, followed by DOX-NP, and free DOX. Overall, DOX-GNPs may be a promising carrier for hydrophobic anticancer drugs.

Keywords: Triblock copolymer; gold cross-linking; biostable nanoparticle; biocompatibility

RSC Advances Accepted Manuscript

Introduction

Cancer is one of the most common causes of death, taking 7 million lives each year worldwide.[1] Although advances in chemotherapy have improved the survival rate of patients over the last few decades, chemotherapeutic agents are generally cytotoxic to normal cells in the body. Often, a large percentage of the cytotoxic drugs administered to the patient does not reach the tumor, but rather is ubiquitously distributed throughout the body, resulting in toxic side effects.[1-2] Polymeric nanoparticles (PNPs) have received substantial attention over the past few decades as drug delivery vehicles because they offer a promising approach to maximize the therapeutic efficacy of a drug without significant side effects.[2-5] These PNPs can accumulate in solid tumors via the enhanced permeation and retention (EPR).[5-8] In traditional PNP systems, however, premature release of the drug prior to reaching the target site often occurs due to poor stability in biological media.[8-12] Therefore, numerous PNPs with high stability have recently been developed, in which either their cores or shells have been covalently cross-linked.[12-16] Although covalent cross-linking of PNPs can improve their stability, they are often prepared using complicated chemistry and toxic fragments are produced by degradation of the organic cross-linkers. In recent years, mineralization of PNPs has been demonstrated as the promising approach to improve their stability.[17,18] However, its biocompatibility and biodegradability are not fully understood yet.

For biomedical applications, polymers have frequently been combined with inorganic nanoparticles, such as gold, silver, quantum dot, and magnetic particles. [16,19-22] In particular, gold nanoparticles (AuNPs) have received increased attention for drug delivery applications, due to their biocompatibility and facile modification.[22-28] However, there are few reports on the development of cross-linked micelles for anticancer drug delivery by AuNPs.[29] In this study, we

RSC Advances Accepted Manuscript

aimed to prepare gold cross-linked PNPs (GCPNPs) that could serve as robust nanocarriers of an anticancer drug. The triblock copolymer, composed of poly(ε-caprolactone)-*block*-poly(2-(dimethylamino) ethyl methacrylate)-*block*-poly(ethylene glycol) (PCL-*b*-PDMAEMA-*b*-PEG), was synthesized to obtain a polymeric amphiphile that can self-assemble into nano-sized particles and allow for the growth of AuNPs inside the particle. Hydrophilic PEG was chosen to prolong the systemic circulation of PNPs, while hydrophobic PCL was used to induce the formation of the nanoparticle core that serves as the reservoir of the hydrophobic drug, DOX. The PDMAEMA block was used as the self-reducing substrate in the gold cross-linking reaction. The DOX-loaded GCPNPs were characterized using various instruments, including transmission electron microscopy (TEM) and dynamic light scattering (DLS). The *in vitro* release of DOX from GCPNPs was monitored as a function of time. In addition, to observe the pharmacokinetics, the DOX concentration in blood was evaluated as a function of time after systemic administration of DOX-GCPNPs into rats. To the best of our knowledge, this is the first report on the use of GCPNPs based on a triblock copolymer as a carrier of a hydrophobic anticancer drug.

Experimental

Materials

2-(Dimethylamino) ethyl methacrylate (DMAEMA) was used after column purification to remove an inhibitor, hydroquinone. DOX, ε-caprolactone (MW = 5 kDa), 2-hydroxyethyl 2-bromoisobutyrate (HEBIB), tin(II) 2-ethylhexanoate $Sn(Oct)_2$, copper(II) bromide ($CuBr_2$), tris[2-(dimethylamino)ethyl]amine (ME_6TREN), sodium azide (NaN_3), PEG methyl ether (MW = 5 kDa), 4-pentynoic acid, 4-(dimethylamino) pyridine (DMAP), *N*,*N*′-

RSC Advances Accepted Manuscript

dicyclohexylcarbodiimide (DCC), *N*,*N*,*N*′,*N*″,*N*″-pentamethyldiethylenetriamine (PMDETA), copper(I) bromide (CuBr), gold(III) chloride trihydrate ($HAuCl_4 \cdot 3H_2O$, 99%), triethylamine (TEA), toluene, dimethylformamide (DMF), dichloromethane (DCM) and tetrahydrofuran (THF) were purchased from Sigma-Aldrich Co. (St. Louis, MO, USA). Squamous cell carcinoma (SCC7) cells were purchased from the American Type Culture Collection (Rockville, MD, USA). For cell culture, RPMI-1640 media, fetal bovine serum (FBS), trypsin-EDTA and Dulbecco's phosphate buffered saline (DPBS) were purchased from WelGENE Inc. (Daegu, Korea). All other solvents were reagent grade and used without further purification.

Synthesis of PCL-Br

The PCL homopolymer was synthesized by ring opening polymerization (ROP) of ε-caprolactonas, as described in the previous report.[30] 5 g of ε-caprolacton (43.8 mmol), 184.88 mg of HEBIB (0.876 mmol), and 20 mL of toluene were added to an oven-dried Schlenk flask under nitrogen. The mixture was stirred and degassed by three consecutive freeze-pump-thaw cycles. Then, 53.23 mg of $Sn(Oct)_2$ (0.1314 mmol) in 5 mL of toluene was added to the flask through a gas-tight syringe. Polymerization was performed at 100 ºC for 24 h. The resulting polymer (PCL-Br) was isolated by precipitation over cold ether, filtered under vacuum and dried under vacuum at room temperature.

Synthesis of PCL-*b*-PDMAEMA- N_3 diblock copolymer

PCL-*b*-PDMAEMA-Br diblock copolymer was synthesized by atom transfer radical polymerization (ATRP) using PCL-Br as the macroinitiator.[31] One gram of PCL-Br (0.1545 mmol), 34.5 mg of $CuBr_2$ (0.1545 mmol), 35.6 mg of ME_6TREN (0.1545 mmol) and 607.2 mg

RSC Advances Accepted Manuscript

of DMAEMA (3.8625 mmol) were dissolved in 10 mL of DMF/toluene co-solvent (1v/1v) in a 25-mL oven-dried Schlenk flask. The mixture was stirred and degassed by three consecutive freeze-pump-thaw cycles. Thereafter, 125.18 mg of $Sn(Oct)_2$ (0.309 mmol) in 1 mL of DMF/toluene co-solvent (1v/1v) was added to initiate polymerization. Polymerization was carried out at 60 ºC for 6 h. The resulting solution was diluted with DCM and passed through a basic alumina column to remove copper from the product solution. The product was concentrated on a rotary evaporator and precipitated in cold ether, filtered and dried under vacuum at room temperature.

To prepare the azide-ended diblock copolymer, 1 g of PCL-PDMAEMA-Br (0.1054 mmol) and 68.56 mg of NaN_3 (1.054 mmol) were dissolved in 10 mL of DMF/THF co-solvent (2v/1v) in a 100-mL oven-dried round bottom flask. The mixture was stirred vigorously for 24 h at room temperature, and purified by dialysis against distilled water for 2 days using a cellulose membrane (MWCO = 3,500 Da, Spectrum®, Rancho Dominquez, CA, USA). The resulting solution was lyophilized to yield PCL-PDMAEMA-N_3.

Synthesis of alkyne-PEG

Alkyne-functionalized PEG was prepared as reported previously.[32] In brief, 2 g of monomethyl PEG (0.4 mol), 81.75 mg of 4-pentynoic acid (1.2 mmol) and 9.8 mg of DMAP (0.08 mmol) were dissolved in 25 mL of DCM in a round bottom flask under nitrogen. The mixture was cooled to 0 ºC, and 247.6 mg of DCC (1.2 mmol) in 5 mL DCM was added dropwise. Then, the mixture was stirred at room temperature for 1 h and allowed to warm to room temperature and stirred for 24 h. The *N*,*N*'-dicyclohexylurea, a byproduct of the reaction, was removed by filtration. The filtrate was washed with DCM, concentrated on a rotary

RSC Advances Accepted Manuscript

evaporator, and purified by dialysis against excess methanol for 2 days using a cellulose membrane (MWCO = 3,500 Da). Thereafter, the resulting solution was precipitated in cold ether, filtered under vacuum and dried under vacuum at room temperature to obtain alkyne-PEG.

Synthesis of PCL-*b*-PDMAEMA-*b*-PEG triblock copolymer

PCL-*b*-PDMAEMA-N_3 (1 g, 0.105 mmol), alkyne-PEG (1.1 g, 0.211 mmol) and PMDTA (36.5 mg, 0.211 mmol) were dissolved in 40 mL THF under nitrogen in a prepared Schlenk flask "**A"**. The mixture was further degassed by three consecutive freeze-pump-thaw cycles. Then, 30.25 mg of CuBr (0.211 mmol) was added in another Schlenk flask "**B"** under nitrogen. The degassed mixture from flask "**A"** was transferred into flask "**B"** via a cannula. The reaction was stirred at 60 ºC for 24 h, and then passed through a basic alumina column to remove copper from the solution. The reaction mixture was concentrated into a pasty mass, and precipitated in cold diethyl ether. The resulting product was collected by suction filtration. The product was redissolved in THF and purified by dialysis against distilled water for 2 days using a cellulose membrane (MWCO = 6-8 kDa) to remove excess PEG. The solution was lyophilized to yield PCL-*b*-PDMAEMA-*b*-PEG**.**

Preparation of DOX-loaded GCPNPs

DOX was loaded into PNPs using a simple dialysis method performed under dark conditions. DOX·HCl (32.55 mg) and TEA (6 mL) were dissolved in 10 mL DMF/distilled water (3v/1v) and mixed with 30 mL of the same co-solvent containing 293 mg triblock copolymer. Then, 40 mL of distilled water was added dropwise with sonication using a probe-type sonicator (VCX-750, Sonics &Materials, CT, USA) and purified by dialysis against distilled water for 1

RSC Advances Accepted Manuscript

day using a cellulose membrane (MWCO = 6-8 kDa). The resulting solution was filtered using a 0.8-μm syringe filter and lyophilized to yield DOX-loaded PCL-*b*-PDMAEMA-*b*-PEG (DOX-PNP).

For the optimization of the gold cross-linking system, various molar ratios of $HAuCl_4 \cdot 3H_2O$ were treated with the tertiary amine of DOX-PNP. In brief, 2 mg of DOX-PNP in 2 mL of distilled water was mixed with the $HAuCl_4 \cdot 3H_2O$ solution, in which the molar ratio of $HAuCl_4$ to the tertiary amine was adjusted in the range of 0.1-3.0. The mixture was stirred at 40 °C for 12 h, centrifuged at 15000 *g* for 30 min, and lyophilized to yield gold cross-linked DOX-PNP (DOX-GCPNP).

Characterization

All polymers were completely characterized using ^{1}H NMR (400 MHz Spectrometer, Bruker Biospin GmbH, Germany) for which the samples were dissolved in C*D*Cl$_3$. The amount of loaded DOX in PNP was determined using a UV/VIS spectrometer (G1103A, Agilent, USA) by measuring absorbance at 490 nm. In brief, DOX-PNP in DMSO/distilled water (1v/1v, 1 mg mL^{-1}) was analyzed based on a standard curve of free DOX. The loading efficiency and loading content of DOX were calculated using the following method:

Loading content (%) = (weight of the loaded drug / weight of the polymer) × 100%

Loading efficiency (%) = (weight of the loaded drug / weight of drug in feed) × 100%

The average diameters of PNP, DOX-PNP and DOX-GCPNP were measured by DLS (Malvern Zetasizer Nano ZS, Malvern, UK). To find the average diameter, all samples were dispersed in PBS (pH 7.4) and sonicated for 3 min using a probe-type sonicator. The morphology

RSC Advances Accepted Manuscript

of the nanoparticles was confirmed by using TEM (CM30, Philips, USA). For TEM measurements, all samples were dispersed in distilled water and stained with 0.5% uranyl acetate.

The stabilities of DOX-PNP and DOX-GCPNP were estimated by measuring the particle size as a function of time, using samples dispersed in PBS (pH 7.4) with or without 20% (v/v) FBS at 37 °C.

In vitro drug release behavior of DOX-GCPNP

In vitro DOX release from DOX-PNP and DOX-GCPNP was carried out at 37 °C in PBS (pH 7.4). In brief, DOX-loaded nanoparticles (2 mg) were dispersed in 2 mL of PBS (pH 7.4) and placed on the dialysis membrane (MWCO = 6-8 kDa). Then, the membrane was immersed in 20 mL of PBS (pH 7.4), and shaken in a 37 °C water bath at 100 rpm. At various time intervals, the medium was replaced with 20 mL of fresh medium to maintain the sink condition. The amount of DOX released was determined, based on a standard curve of free DOX, using a microplate reader (VERSAmaxTM, Molecular Devices Corp, Sunnyvale, CA).

In vitro cell viability test of DOX-GCPNP

SCC7 cells were cultured in RPMI 1640 medium containing 10% (v/v) FBS and 1% (v/v) penicillin-streptomycin at 37 °C in a CO_2 incubator. The cytotoxic effects of PNP, GCPNP, DOX-PNP and DOX-GCPNP in SCC7 cells were evaluated using a cell counting kit (CCK) assay. In brief, 5×10^3 SCC7 cells were seeded in a 96-well culture dish and allowed to stabilized for 24 h. The cells were then washed twice with DPBS and incubated for 24 h in medium containing various concentrations of the sample. Thereafter, the medium was replaced

RSC Advances Accepted Manuscript

by 200 μL of a CCK solution (10 v/v% in RPMI medium) and incubated for 1 h at 37°C. The supernatant was then analyzed using a microplate reader to measure absorbance at 450 nm.

In vitro cellular uptake of DOX-GCPNP

SCC7 cells (1×10^5 cells/well) were seeded on gelatin-coated cover slips in 6-well plates and allowed to stabilized for 24 h. The cells were then treated with DOX-loaded nanoparticles (10 μg mL^{-1} of DOX) in serum-free RPMI 1640 medium for 3 or 24 h at 37 °C. Afterwards, the cells were washed twice with DPBS (pH 7.4) and fixed with a 4% paraformaldehyde solution for 10 min. The nuclei were stained using 4,6-diamino-2-phenylinodole for 10 min at room temperature, and the intracellular localization of DOX was observed using an IX81-ZDC focus drift compensating microscope (Olympus,Tokyo, Japan).

In vivo pharmacokinetics of doxorubicin

Free DOX (5 mg kg^{-1}), DOX-PNP (DOX 5 mg kg^{-1}), or DOX-GCPNP (DOX 5 mg kg^{-1}) was intravenously administered into male Sprague–Dawley rats (average body weight = 200 g) through the tail vein (n = 3 rats per each group). After intravenous injection of the sample, blood samples (500 μL) were collected at different time points and mixed with 3.8% sodium citrate solution. Plasma was obtained by centrifuging blood at 6000 g for 3 min at 4 °C, and was then stored at −70 °C. DOX was extracted from the plasma, according to the procedure described previously.[33] The quantity of DOX in the plasma was measured using a microplate reader with excitation at 470 nm and emission at 590 nm.

RSC Advances Accepted Manuscript

Results and discussion

Synthesis and characterization

To obtain a biostable nanocarrier, GCPNPs were prepared by growing AuNPs in the core of DOX-loaded PNPs (Fig. 1a). Towards this goal, PCL-*b*-PDMAEMA-*b*-PEG was synthesized by ATRP of DMAEMA in the presence of PCL-Br as the macroinitiator, followed by conjugation of alkyne-PEG via click chemistry (Fig. 1b). To prepare the triblock copolymer, the macroinitiator PCL-Br as was first synthesized by ROP of ε-caprolactone in the presence of hydroxyisobutyryl bromide. In the ^{1}H NMR spectrum of PCL-Br, there was no peak at 3.60 ppm, which would appear from the hydroxyl group of hydroxyisobutyryl bromide. The characteristic peaks appeared due to the presence of methylene groups (4.20 ppm and 1.65 ppm) in PCL and the methyl group (1.90 ppm) of hydroxyisobutyryl bromide, thereby indicating the formation of PCL-Br by the esterification reaction between ε-caprolactone and hydroxyisobutyryl bromide (see ESI, Fig. S1a†). The structure of PCL-*b*-PDMAEMA-Br was also confirmed by ^{1}H NMR, as shown in Fig. S1b†, e.g., 2.60 ppm (NCH_2- in the DMAEMA residue), 1.65 ppm (the middle -CH_2- protons in the PCL residue) and 1.0 ppm (N(CH_3)$_2$- in the DMAEMA residue). The molecular weight of PCL-*b*-PDMAEMA-Br, estimated by integration of the characteristic peaks in ^{1}H NMR, was 9071 g mol^{-1} (see ESI, Table S1†). From the FT-IR spectrum of PCL-*b*-PDMAEMA-N_3, the peak at 2100 cm^{-1} appeared due to the presence of the stretching frequency of azide (see ESI, Fig. S2†). After synthesis of PCL-*b*-PDMAEMA-N_3 and alkyne-PEG, click chemistry was employed in the presence of copper (II) bromide to prepare the triblock copolymer. The chemical structure of PCL-*b*-PDMAEMA-*b*-PEG was characterized by ^{1}H NMR and FT-IR. For the triblock copolymer, the characteristic peak of PEG was observed at 3.6 ppm

RSC Advances Accepted Manuscript

(-CH_2-CH_2-O-) (see ESI, Fig. S1c†). Also, in the FT-IR spectrum, the disappearance of the azide signal at 2095 cm^{-1} in the PCL-*b*-PDMAEMA-*b*-PEG copolymer confirmed the successful click reaction (see ESI, Fig. S2†).

PDMAEMA has been demonstrated to act as a precursor in the production and growth of AuNPs in the network.[34-35] Therefore, we attempted to deposit AuNPs *in situ* in the core of DOX-PNPs using the PDMAEMA block as the reducing substrate (Fig. 1). The reduction of $HAuCl_4$ occurs through the transfer of electrons from the tertiary amine groups present in PDMAEMA of DOX-PNP to the Au^{3+} ion, leading to formation of Au^0. Thereafter, this metallic gold nucleates and grows to form AuNPs, which are stabilized by the PDMAEMA chain.[34] This technique allows for control over the size of AuNPs by varying the feed ratio of PDMAEMA and $HAuCl_4$. Also, AuNPs are evenly distributed without stabilizer in the core of PNPs during the reaction. The optical properties of AuNPs in the core of PNPs were observed by varying the feed ratio of $HAuCl_4$ to PDMAEMA. As presented in Fig. 2a, the reddish color of the GCPNPs was enhanced as the feed ratio increased for ratios up to 1. At a feed ratio higher than 1, the solution became a dark violet color, indicating aggregation of AuNPs. The presence of embedded AuNPs in the cores of the DOX-PNPs was also confirmed by UV/VIS spectral analysis (Fig. 2b). The spectrum for GCPNPs with a feed ratio of 1 revealed a band at 530 nm, implying the presence of AuNPs. However, GCPNPs with a feed ratio of 1.5 exhibited a broader band at 550 nm, due to the existence of aggregated AuNPs.[35] For all additional experiments, GCPNPs with a feed ratio of 1 were used because the UV/VIS results implied that they contain AuNPs without aggregation.

The size distributions and morphologies of PNPs, DOX-PNPs and DOX-GCPNPs are shown in Fig. 3. DLS was used to measure the hydrodynamic size of the nanoparticles, and their morphology was determined by TEM. The PNPs were spherical in shape, with a size of 195 nm.

RSC Advances Accepted Manuscript

Their size decreased to 168 nm after encapsulation of DOX, implying the formation of compact nanoparticles. The installation of AuNPs in DOX-PNPs slightly decreased the size to 156 nm. The TEM images of DOX-GCPNPs demonstrated the even distribution of AuNPs in the core of the nanoparticles, implying that AuNPs may contribute to the stability of nanoparticles and act as a diffusion barrier for DOX.

***In vitro* stability and drug release behavior of DOX-GCPNPs**

To assess the stability of the nanoparticles, particle sizes were measured in PBS (pH 7.4) for 5 days as a function of time (Fig. 4a). DOX-PNPs showed a drastic increase in the size, resulting in the formation of 2.3-fold larger nanoparticle in 5 days. Interestingly, DOX-GCPNPs did not show a significant change in the size, suggesting their high stability. We also monitored changes in particle sizes in the presence of 20% (v/v) FBS to evaluate whether nanoparticles can maintain a stable structure upon interaction with serum. As presented in Fig. 4b, the particle size of DOX-PNPs rapidly increased to 390 nm in 3 h, which may have been due to ionic interactions between the positively charged PDMAEMA block and the negatively charged proteins in FBS. It is worth noting that the DOX-GCPNPs showed little change in the size, implying that the stability of the nanoparticles was enhanced by the installation of AuNPs.

To investigate the effect of AuNPs in GCPNPs on drug release, DOX was chosen as a model anticancer drug. Fig. 5a shows the DOX release profile from DOX-PNPs and DOX-GCPNPs under physiological conditions (PBS, pH 7.4). Both DOX-PNPs and DOX-GCPNPs showed a burst release of DOX for one day, followed by sustained release for the remaining time evaluated. Most of the DOX (>80%) was released from PNPs over 6 days, whereas only 42% of the DOX was released from GCPNPs. The slow release of DOX from GCPNPs may have been

RSC Advances Accepted Manuscript

due to the presence of AuNPs that acted as a diffusion barrier. The physical interaction between the surface of the AuNPs and DOX may also have been responsible for its slow release from GCPNPs.

The *in vitro* cytotoxicities of PNPs, GCPNPs, DOX-PNPs and DOX-GCPNPs were evaluated using the CCK assay. We confirmed that PNPs resulted in no toxicity at concentrations up to 500 μg mL^{-1} and that the introduction of AuNPs resulted in no distinguishable effect on the toxicity of the nanoparticles (see ESI, Fig. S3†). As shown in Fig. 5b, DOX-PNPs and DOX-GCPNPs caused dose-dependent cytotoxicity. Interestingly, DOX-PNPs exhibited significantly higher cytotoxicity than DOX-GCPNPs, which may have been due to the sustained release of DOX from GCPNPs. This result is in good agreement with the release behavior of DOX shown in Fig. 5a.

In vitro cellular uptake of DOX-PNPs and DOX-GCPNPs

To observe the cellular uptake behavior of DOX, SCC7 cells were treated with DOX-PNP and DOX-GCPNP and monitored using confocal microscopy (Fig. 6). A strong fluorescent signal from DOX, resulting from release of DOX, was observed in the cytosol of the cells after they were treated for 24 h with DOX-PNP and DOX-GCPNP. Of note, the cells treated with DOX-PNP exhibited a stronger fluorescent signal than those treated with DOX-GCPNP. This finding may have been due to the slower release of DOX in the presence of AuNPs, which act as a diffusion barrier. We further visualized the uptake of AuNPs in DOX-GCPNPs in cancer cells, using dark field microscopy, and demonstrated that the amount of internalized AuNPs increased as a function of incubation time.

RSC Advances Accepted Manuscript

In vivo pharmacokinetics

The *in vivo* pharmacokinetics of DOX-loaded nanoparticles were evaluated by measuring DOX concentration in blood after intravenous injections into the tail veins of rats. As shown in Fig. 7, free DOX completely disappeared from blood 12 h post-injection, whereas the fluorescent signal of DOX in PNPs was detectable for up to 48 h. Interestingly, DOX-GCPNPs remained in the blood 72 h post-injection. At 12 h, the DOX concentration in blood obtained from rats treated with DOX-GCPNPs, was 12.3-fold and 1.6-fold higher than those measured in rats treated with free DOX or DOX-PNPs, respectively (Fig. 7). The half-lives of free DOX, DOX-PNPs and DOX-GCPNPs were 1.95 h, 5.37 h and 9 h, respectively. We therefore conclude that DOX-GCPNPs with a stable cross-linked structure exhibit prolonged blood circulation, which may increase the probability of delivering drug to the tumor site. Overall, compared to the conventional approaches to improve the biostablity of NPs such as covalent cross-linking and mineralization, gold cross-linking might be useful to prepare the biostable NPs because it could be achieved without producing toxic fragments and by a facile procedure.

Conclusion

The triblock copolymer, composed of PCL-*b*-PDMAEMA-*b*-PEG, was synthesized by a combination of ROP, ATRP, and click chemistry. Due to the amphiphilic nature of the triblock copolymer, it formed nano-sized spherical particles (195 nm in diameter) in an aqueous environment. DOX was effectively loaded into PNPs using a simple dialysis method. The tertiary amine groups, present in PDMAEMA of the triblock polymer, were used for *in situ* gold cross-linking. The GCPNPs showed no significant changes in particle size under serum conditions, indicating high biostability. DOX was released from GCPNPs in a sustained manner,

RSC Advances Accepted Manuscript

likely due to the presence of AuNPs, which acted as a diffusion barrier. The pharmacokinetic results indicated that the high stability of DOX-GCPNPs significantly increased the blood circulation time of DOX. Overall, gold cross-linked nanocarriers may have promising potential as a drug carrier system for DOX.

Acknowledgments

This work was financially supported by the National Research Council of Science and Technology (NST) through the Degree and Research Center (DRC) Program (2014), and the Basic Science Research Programs (20100027955 & 2015R1A2A2A05001390) of MSIP. J. H. Park gratefully acknowledges the support from LG Yonam Foundation.

Electronic supplementary information (ESI)

† Electronic supplementary information (ESI) available: Reaction conditions, ^{1}H NMR, FT-IR, and cytotoxicity of triblock copolymer.

References

1. A. Jemal, R. Siegel, J. Xu, and E. Ward, *CA-Cancer J. Clin*., 2010, **5**, 277-300.
2. R. Duncan, *Nat. Rev. Drug Discov.*, 2003, **2**, 347-360.
3. R. Duncan, *Nat. Rev. Cancer*, 2006, **6**, 688-701.
4. R. Duncan and J. Kopecek, *Adv. Polym. Sci.*, 1984, **57**, 51-101.
5. V. N. Rao, S. R. Mane, A. Kishore, J. Das Sarma and R. Shunmugam, *Biomacromolecules,* 2012, **13,** 221-230.
6. V. N. Rao, Naidu, S. Sarkar, J. Das Sarma, R. Shunmugam, *Bioconjugate Chem.*, 2014, **25**, 276-285
7. A. K. Singla, A. Garg and D. Aggarwal, *Int. J. Pharm.*, 2002, **235**, 179-192.
8. J. M. Stukel, R. C. Li, H. D. Maynard and M. R. Caplan, *Biomacromolecules,* 2010, **11**, 160-167.

RSC Advances Accepted Manuscript

9. T. Lammers, S. Aime, W. E. Hennink, G. Storm and F. Kiessling, *Acc. Chem. Res.*, 2011, **44**, 1029-1038.
10. J. Shi, A. R. Votruba, O. C. Farokhzad and R. Langer, *Nano Lett.*, 2010, **10**, 3223-3230.
11. R. K. O'Reilly, C. J. Hawker and K. L. Wooley, *Chem. Soc. Rev.*, 2006, **35**, 1068-1083.
12. E. S. Read and S. P. Armes, *Chem. Commun.*, 2007, **29**, 3021-3035.
13. H. Xu, F. Meng and Z. Zhong, *J. Mater. Chem.*, 2009, **19**, 4183-4190.
14. R. Cheng, F. Meng, S. Ma, H. Xu, H. Liu, X. Jing and Z. Zhong, *J. Mater. Chem.*, 2011, **21**, 19013-19020.
15. J. S. Katz, D. H. Levine, K. P. Davis, F. S. Bates, D. A. Hammer and J. A. Burdick, *Langmuir*, 2009, **25**, 4429-4434.
16. M. J. Joralemon, S. McRae and T. Emrick, *Chem. Commun.*, 2010, **46**, 1377-1393.
17. S. Y. Han, H. S. Han, S. C. Lee, Y. M. Kang, I. S. Kim and J. H. Park, *J. Mater. Chem.*, 2011, **21**, 7996-8001.
18. H. S. Han, J. Lee, H. R. Kim, S.Y. Chae, M. Kim, G. Saravanakumar, H. Y. Yoon, D. G. You, H. Ko, K. Kim, I. C. Kwon, J. C. Park, J. H. Park, *J. Controlled Release.*, 2013, **168**, 105-114.
19. J. Du and R. K. O'Reilly, *Soft Matter*, 2009, **5**, 3544-3561.
20. K. B. Thurmond, T. Kowalewski and K. L. Wooley, *J. Am. Chem. Soc.*, 1996, **118**, 7239-7240.
21. R. J. Thibault, O. Uzun, R. Hong and V. M. Rotello, *Adv. Mater.*, 2006, **18**, 2179-2183.
22. P. Ghosh, G. Han, M. De, C. K. Kim and V. M. Rotello, *Adv. Drug Delivery Rev.*, 2008, **60**, 1307-1315.
23. M. S. Yavuz, Y. Cheng, J. Chen, C. M. Cobley, Q. Zhang, M. Rycenga, J. Xie, C. Kim, K. H. Song, A. G. Schwartz, L. V. Wang and Y. Xia, *Nat. Mater.*, 2009, **8**, 935-939.
24. A. Kyrsting, P.M. Bendix, D.G. Stamou, and L. B. Oddershede, *Nano Lett.*, 2011, **11**, 888-892.
25. A. M. Alkilany, L. B. Thompson, S. P. Boulos, P. N. Sisco and C. J. Murphy, *Adv. Drug Delivery Rev.*, 2012, **64**, 190-199.
26. A. Elbakry, A. Zaky, R. Liebl, R. Rachel, A. Goepferich and M. Breunig, *Nano Lett.*, 2009, **9**, 2059-2064.
27. H. Park, H. Tsutsumi and H. Mihara, *Biomaterials*, 2014, **35**, 3480-3487.
C. K. Kim, P. Ghosh, C. Pagliuca, Z. J. Zhu, S.Menichetti, V .M. Rotello, *J. Am. Chem. Soc.*, 2009, **131**, 1360-1361.
28. K. H. Bae, S. H. Choi, S. Y. Park, Y. Lee and T. G. Park, *Langmuir*, 2006, **22**, 6380–6384.
29. Y. Tao, J. Han, C. Ye, T. Thomas and H. Dou, *J. Mater. Chem.*, 2012, **22**, 18864.
30. L. J. Bai, L. F. Zhang, Z. P. Cheng and X. L. Zhu, *Polym. Chem.*, 2012, **3**, 2685-2697.
31. W. Jakubowski and K. Matyjaszewski, *Macromol. Symp.*, 2006, **240**, 213-223.
32. Y. Y. Durmaz, M. Sangermano and Y. Yagci, *J. Polym. Sci., Part A: Polym. Chem.*, 2010, **48**, 2862-2868.

RSC Advances Accepted Manuscript

33. H. S. Han, K. Y. Choi, H. Ko, J. Jeon, G. Saravanakumar, Y. D. Suh, D. S. Lee and J. H. Park, *J. Controlled Release*, 2015**, 200,** 158-166.
34. J. D. S. Newman and G. J. Blanchard, *Langmuir*, 2006, **22**, 5882-5887.
35. R. Das, D. Das, P. Ghosh, S. Dhara, A. B. Panda and S. Pal, *RSC Adv.*, 2015, **5**, 27481-27490.

RSC Advances Accepted Manuscript

Table 1. Physicochemical characteristics of PNP, DOX-PNP and DOX-GCPNP.

Sample	Size (nm)[a]	ζ (mV)[b]	DOX loading content (wt%)[c]	DOX loading efficacy (wt%)[d]
PNP	195.4 ± 0.70	35.1 ± 2.21	-	-
DOX-PNP (10 %)	167.7 ± 5.16	29.8 ± 0.95	5.53 ± 0.04	55.3 ± 0.02
DOX-GCPNP (1 : 1)	156.0 ± 1.63	27.1 ± 1.90		

[a]Measured using dynamic light scattering (DLS).
[b]Measured using a zeta-potential analyzer.
[c]Loading content of DOX was calculated using UV/VIS spectrometer.
[d]Loading efficiency (%) = (Loading content of DOX / Feeding content of DOX) × 100(%).

RSC Advances Accepted Manuscript

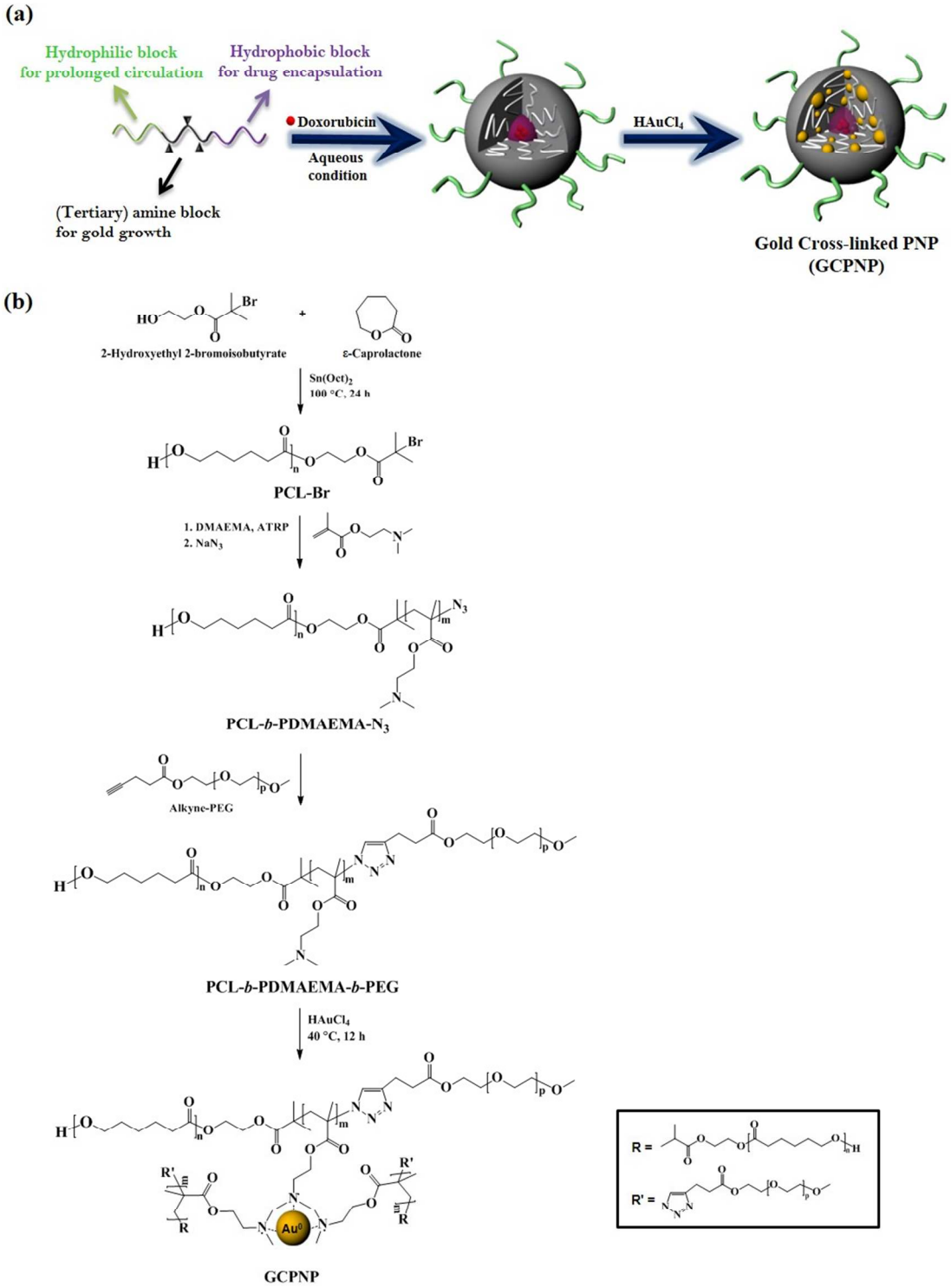

Fig. 1. (a) Schematic illustration of the preparation of DOX-GCPNP and (b) the synthetic route of GCPNP.

RSC Advances Accepted Manuscript

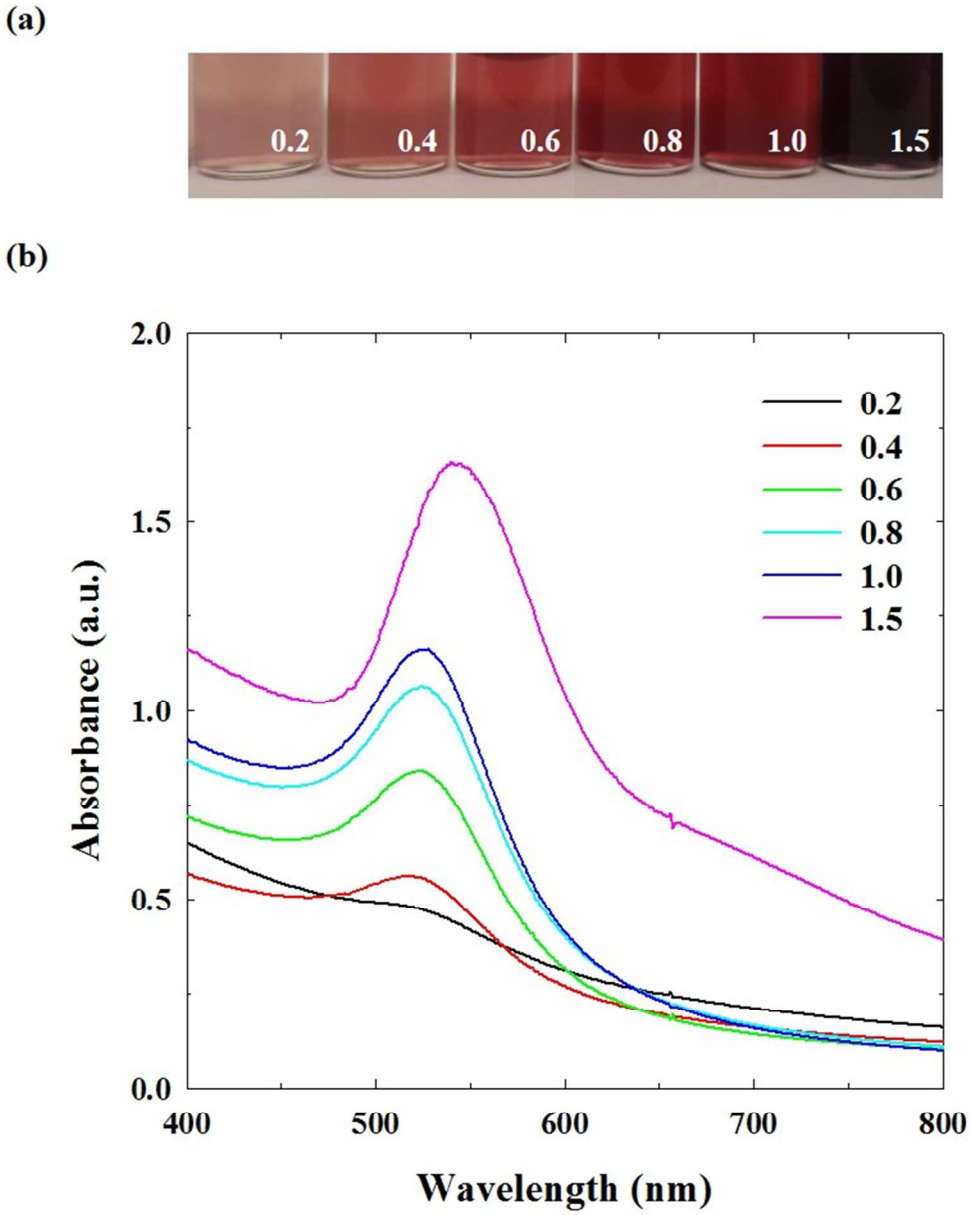

Fig. 2. Formation of AuNPs in PNPs at different feed ratios of $HAuCl_4$ and tertiary amine. (a) Photographs and (b) UV/VIS spectra of the GCPNP solutions.

RSC Advances Accepted Manuscript

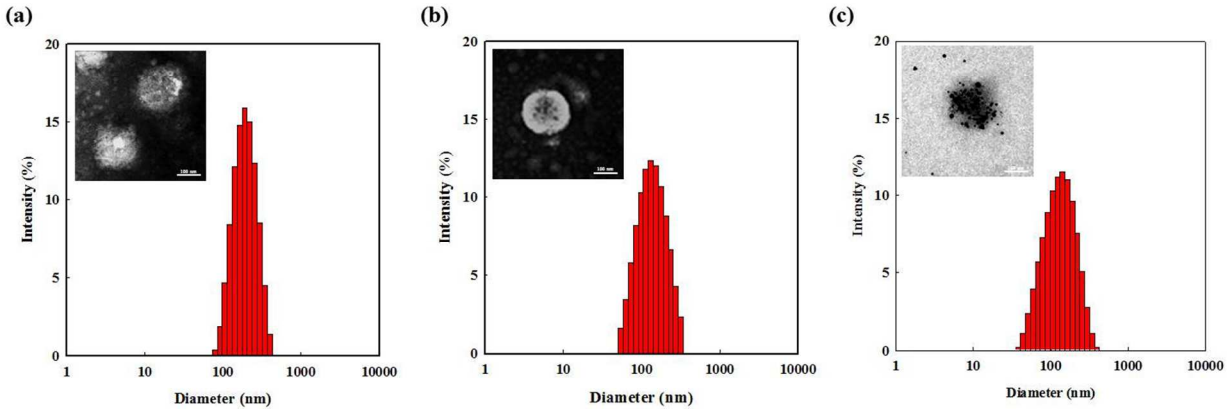

Fig. 3. Size distribution of (a) PNPs, (b) DOX-PNPs and (c) DOX-GCPNPs. The insets are TEM images.

RSC Advances Accepted Manuscript

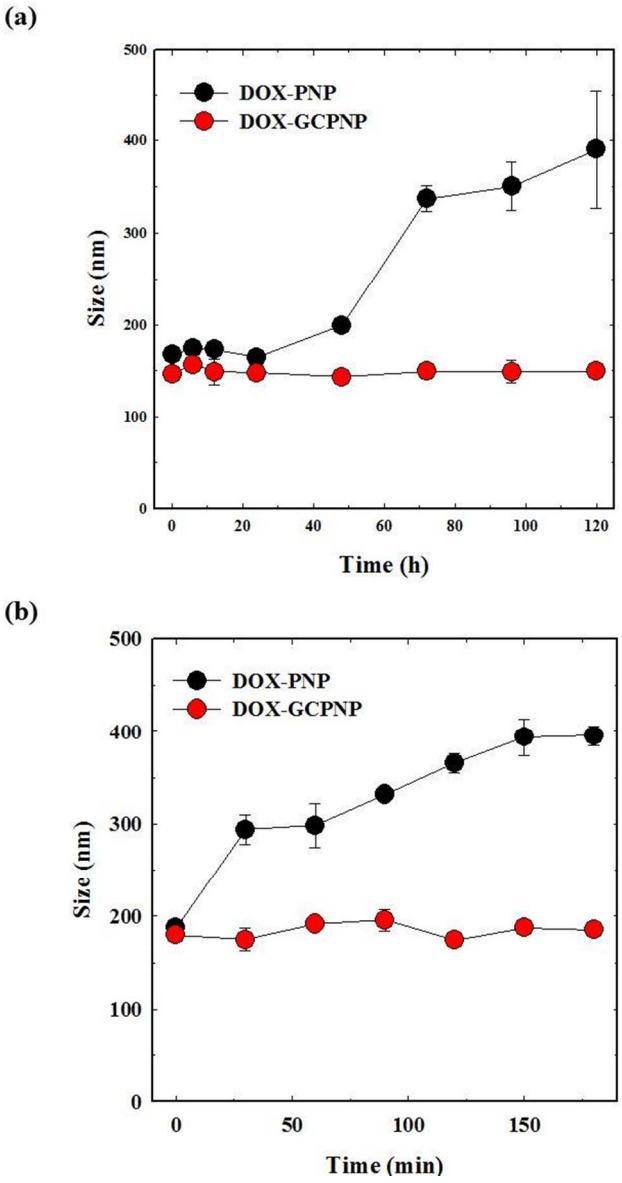

Fig. 4. Stability of DOX-PNPs and DOX-GCPNPs in (a) PBS (pH 7.4) and (b) PBS containing 20% FBS. The error bars in the graph represent standard deviation (*n*=3).

RSC Advances Accepted Manuscript

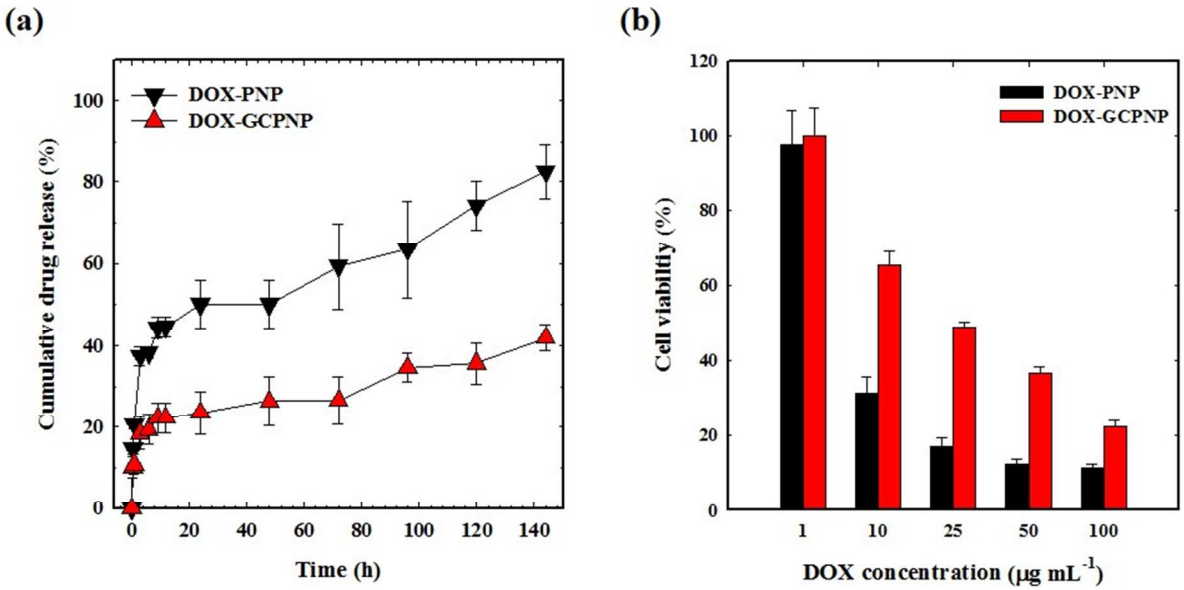

Fig. 5. (a) *In vitro* release behavior of DOX from DOX-PNPs and DOX-GCPNPs and (b) *in vitro* cytotoxicity. The error bars in the graph represent standard deviation (*n*=3).

RSC Advances Accepted Manuscript

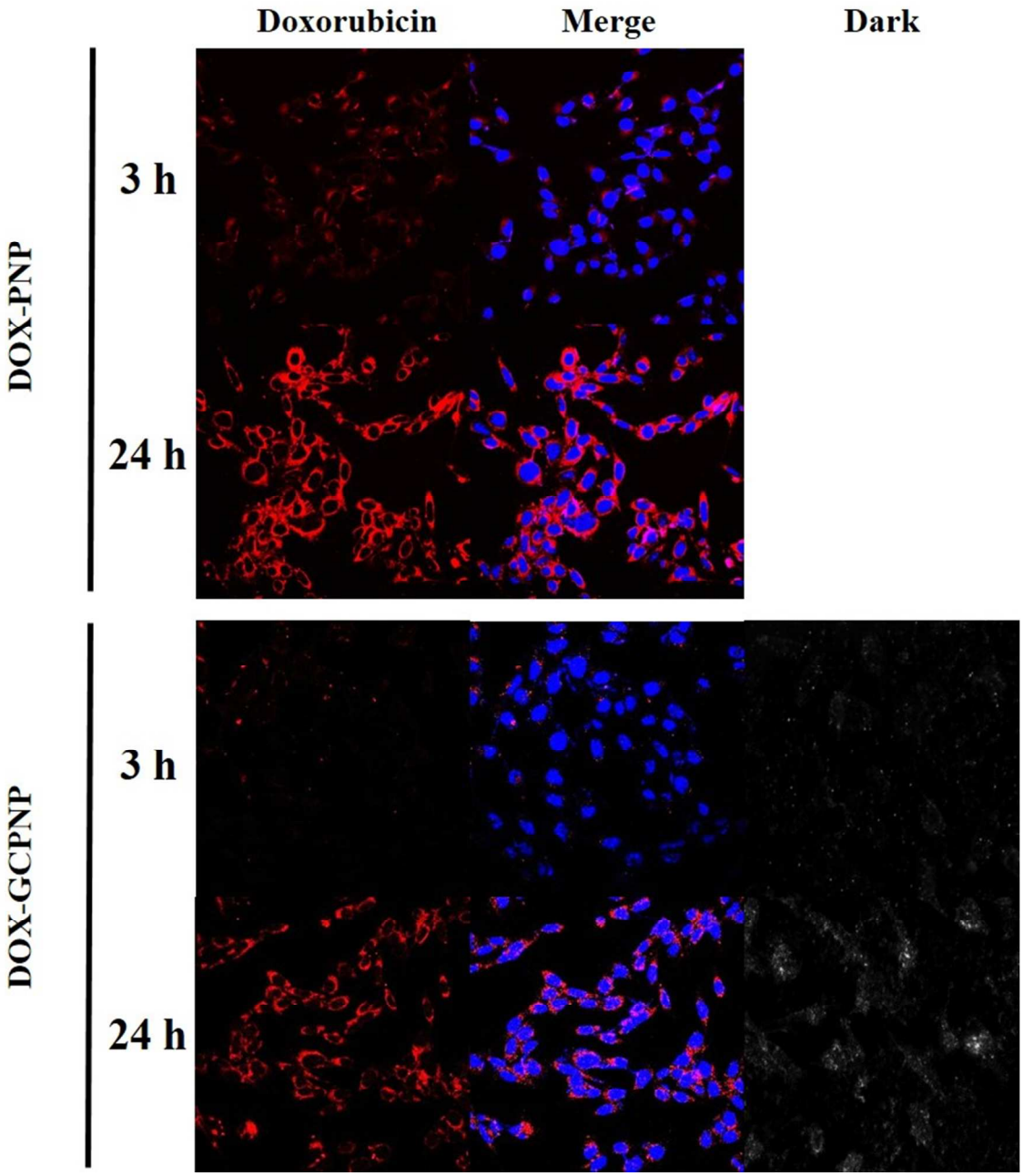

Fig. 6. Cellular uptake of DOX-PNPs and DOX-GCPNPs. SCC7 cells were treated with 10 μg mL^{-1} DOX for 3 or 24 h.

RSC Advances Accepted Manuscript

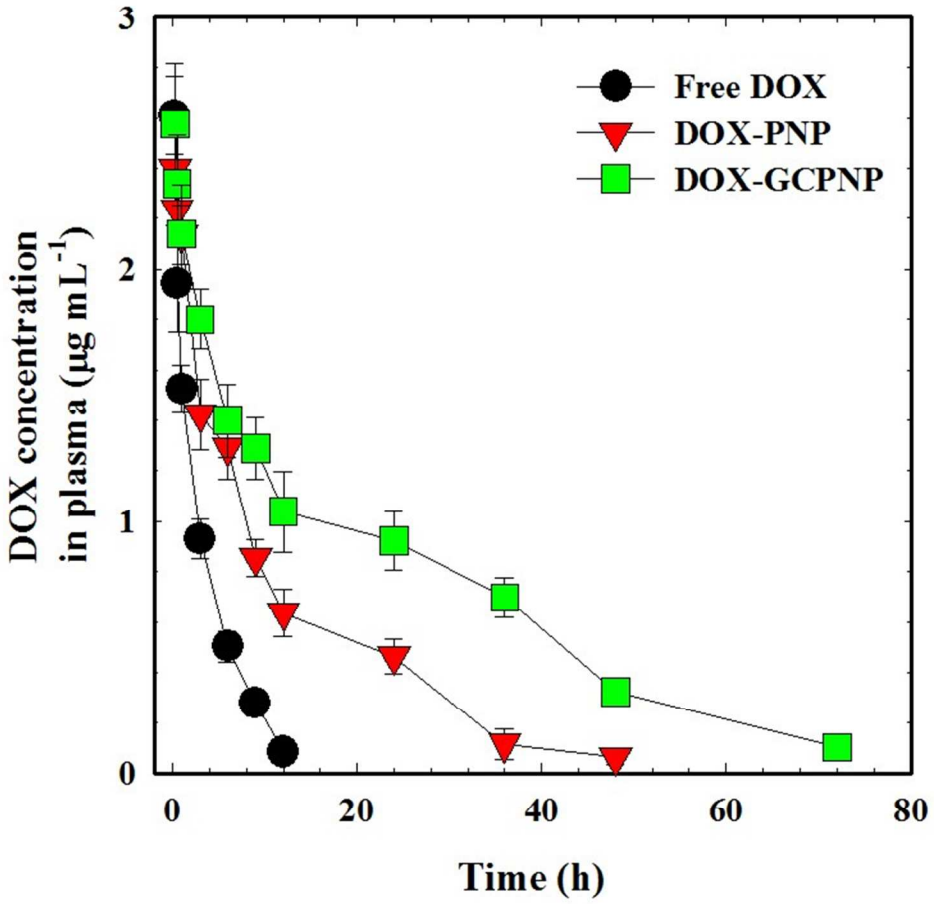

Fig. 7. *In vivo* pharmacokinetics of DOX. The error bars in the graph represent standard deviations (*n*=3).

RSC Advances Accepted Manuscript

Graphical Abstract

Gold cross-linked nanoparticles based on PCL-*b*-PDMAEMA-*b*-PEG triblock copolymer has been developed as a carrier for anticancer drugs with enhanced biostability.

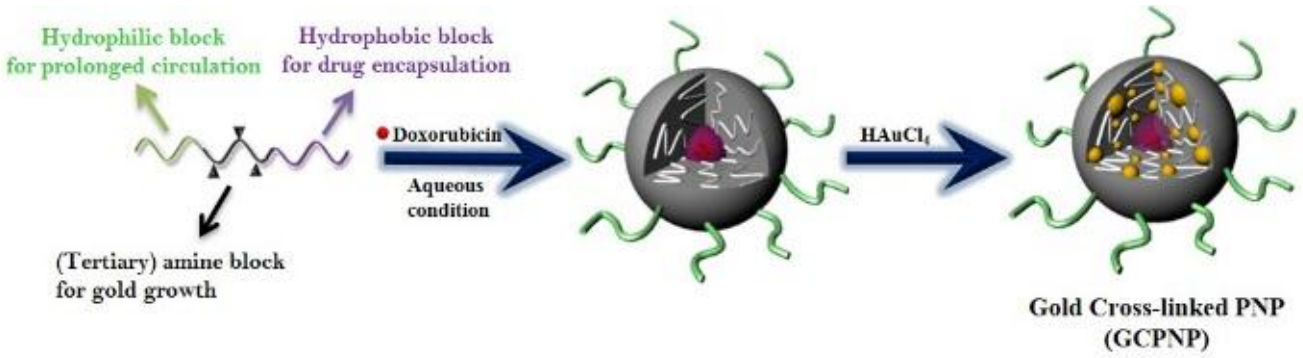

RSC Advances Accepted Manuscript